SCIREA Journal of Clinical Medicine
ISSN: 2706-8870
http://www.scirea.org/journal/CM
May 10, 2020
Volume 5, Issue 2, April 2020

5-tRF-His, tRNA-derived fragments, regulate CKAP2 to inhibit the proliferation of breast cancer

Xun Tang [1], Pan Jiang [1], Huanhuan Chen [1], Jun Wu [2], Xiaodong Xie [3], Xuelian Mao [1], Dongping Mo [1], Li Tang [1], Feng Yan [1*]

[1]Department of Clinical Laboratory, the Affiliated Cancer Hospital of Nanjing Medical University & Jiangsu Cancer Hospital & Jiangsu Institute of Cancer Research, Baiziting Road 42, Nanjing 210009, P. R. China.

[2]Department of Clinical Laboratory, the Affiliated Brain Hospital of Nanjing Medical University, Guangzhou Road 264, Nanjing 210009, P. R. China.

[3]Department of Radiology, the Affiliated Cancer Hospital of Nanjing Medical University & Jiangsu Cancer Hospital & Jiangsu Institute of Cancer Research, Baiziting Road 42, Nanjing 210009, P. R. China.

* Correspondence: yanfeng@jszlyy.com.cn

Abstract

tRNA derived fragments are differentiated expressed in human breast cancer(BC) tissues. Among of them, 5-tRF-His attracted our attention due to its potential role in breast cancer progression. PCR and in situ hybridization were used to measure the expression and location of 5-tRF-His. The role of 5-tRF-His *in vitro* was explored by cell proliferation assays and flow cytometery. The effect of 5-tRF-His *in vivo* was performed by Xenograft experiments and immunohistochemistry. We determined the derivation of 5-tRF-His by northern blot and clarified the mechanism of 5-tRF-His by immunoprecipitation and western blot. We observed that strong downregulation of 5-tRF-His in clinical BC samples. Reduced 5-tRF-His can lead

to lymph node metastasis. 5-tRF-His, a tRNA-derived fragment linked to pan-ago, regulates the proliferation and apoptosis of BC cells and inhibits BC tumor growth explant tumor *in vivo*. The increase in proliferation and the decrease in apoptosis induced by the 5-tRF-His inhibitor were reversed by si-CKAP2. 5-tRF-His inhibits BC development *in vivo and vitro*. The 5-tRF-His/CKAP2/erk2 axis affects the proliferation and apoptosis of BC cells, imply that 5-tRF-His may be a promising tumor marker of BC patients serum and treatment target for BC therapy.

Keywords: breast cancer; serum; tRNA-derived fragments; CKAP2; proliferation; ERK2 signaling pathway

1. Introduction

Breast cancer (BC) has become a global burden of cancer and ranks first in both cancer diagnosis and death notably among females worldwide [1]. Although there has been continued progress in the diagnosis and treatment of BC, high mortality remains a major obstacle [2].

In recent decades, due to the development of sequencing technology, abnormal regulation of small noncoding RNAs, such as microRNAs (miRNAs) and long noncoding RNAs (lncRNAs), was shown related to dysfunctional gene expression, as well as tumourigenesis [3,4]. One class of novel identified small noncoding RNA—tRNA derived fragments (tRFs) was shown to be involved in the occurrence of cancer.

tRFs originally derived from tRNAs are highly conserved across species, suggesting their critical roles. Mature or precursor tRNA is cleaved by various kinds of enzymes including Dicer and Angiogenin [5,6]. On the basis of the splice site, the fragments were divided into the following types: 3'tRF, 5'tRF, tiRNAs, and tRNA halves. Researchers have recently focused on the potential activity of tRFs, especially 3'tRF and 5'tRF, as they have similar lengths as miRNAs [7,8]. Previously, our group reported the intriguing expression profile of tRFs in BC tissues through sequencing technique [9] and among the sequences studied, one type of tRF, named 5-tRF-His, may serve as miRNA in breast cancer.

Cytoskeleton-associated protein 2 (CKAP2) stabilizes microtubules and functions during various biological progresses [10]. Many studies have shown that CKAP2 can result in dysregulated differentiation in various human cancer cells and in other organs through

multiple signalling pathways, such as FAK-ERK2, JAK2-STAT3, and Cyclin A-CDK [11-13]. Furthermore, the prognostic value of CKAP2 was assessed among subgroup analysis of BC, especially HER2-negative luminal BC [14]. Therefore, CKAP2 could serve as an oncogene and potential prognostic marker in cancers.

Nevertheless, the function of 5-tRF-His in BC still remains unknown. The study aimed to explore how this molecule participates in breast tumorigenesis. In this study, we demonstrated a reduction in 5-tRF-His and an increase in CKAP2 expression in BC. The regulatory mechanism between these molecules also provides a target for cancer diagnosis and therapy.

2. Experimental Section

2.1 Tissue and serum samples and cell lines

BC tissues and adjacent normal tissues from 27 BC patients undergoing surgery between November 2018 and May 2019 at The Affiliated Cancer Hospital of Nanjing Medical University (Nanjing, China) were assessed for eligibility. Adjacent normal tissues were obtained five centimetres away from the cancer tissue edge and verified by a pathologist to confirm the lack of tumor cells. None of the patients received chemotherapy or radiotherapy prior to surgery. Twenty healthy controls and sixty BC patients before curative surgery with serum samples were recruited for the study at The Affiliated Cancer Hospital of Nanjing Medical University. Detailed clinical pathological data for each specimen were obtained. The study was conducted according to the Ethics Committee of Nanjing Medical University [NO.471 (2018)], and all patients signed informed consent forms.

A human normal breast cell line (HBL-100), human BC cell lines (MCF7, MDA-MB-231, BT549), human liver cancer cells (SMMC-7721, 7402), and human colorectal cancer cells (HT-29, HCT116) were purchased from the Cell Bank of the Type Culture Collection of the Chinese Academy of Science (Shanghai, China). Human HEK293T cells were acquired from the American Type Culture Collection (ATCC) (Maryland, U.S.A). The cells were cultured in DMEM supplemented with 10% FBS and 1% streptomycin/penicillin.

2.2 RNA extraction, RT-qPCR and, northern blot

Total RNA was extracted by TRIzol (Invitrogen, USA). The isolations from cell nucleus and cytoplasm were obtained by the PARISTM Kit (Invitrogen, USA) complying with the manufacturer’s instructions, and followed by removal of the modifications by the rtDtarTM

tRF&tiRNA Pretreatment Kit (Arraystar, U.S.A). RT-qPCR was experienced as described previously [15], using the following primers: human CKAP2, forward 5’-GTGGTGGGGAAACATTGTATTC-3' and reverse 5’-ATGTTGACTTTGGGGATCATCT-3'; 5-tRF-His, forward 5’-CAGTCCGACGATCTGCCG-3' and reverse 5’-GCTCTTCCGATCTCTAACC--ACTAT-3'; U6, forward 5’-GCTTCGGCAGCACATATACTAAAAT-3' and reverse 5’-CGCTTCACGAATTTGCGTGTCAT-3'. Thirty micrograms of RNA from each sample was used for northern blot. Electrophoresis, membrane transfer, prehybridization, hybridization and development were performed. The sequence of 5-tRF-His probe was 5’-CTAACCACTATACGATCACGGCA-3’, which was labeled by digoxin at the 5’ end (Bersin, Guangzhou).

2.3 Oligonucleotide, lentivirus transfection, and vectors

The 5-tRF-His mimics, inhibitors and small interfering RNA targeting CKAP2 (si-CKAP2) were chemically synthesized by RiboBio (Guangzhou, China). We transfected the cells in accordance with the manufacturer’s protocol. The 293T-control and 293T-shDICER1 stable cell lines were transfected with plasmids purchased from GeneChem (Shanghai, China) and then treated with 2μg/mL puromycin for 2 days. The lentivirus vector of mature tRF (His)-GTG-1-5 was described in supplymentary. CKAP2 (wild-type and mutant 3’UTR)-luciferase reporters were purchased from RiboBio.

2.4 In situ hybridization (ISH), immunohistochemistry (IHC) and western blot

ISH was carried out to measure the expression levels of 5-tRF-His in tissue microarray (TMA) (n=140) slides of BC purchased from Xinchao (Shanghai, China). After deparaffinization and hydrateon, the slides were activated by endogenous enzymes and digested with pepsin. Preybridization, hybridization, washing and blocking were performed. Then, the slides were incubated with or anti-digoxin Fab fragments followed by development with DAB substrate. The digoxin-labelled probe was used as described in the northern blot.

The protein expression of CKAP2 (Abcam, Cat#ab198188) in the TMA and Ki67 (Proteintech, Cat#27309-1-AP) in the isolated tumor slides were analyzed by IHC. During the processing, eight arrays were off the slide. IHC and western blot experiments were performed accordingly as descried in previous study [15-16].

2.5 Immunoprecipitation (IP)

After 1 × 108 MCF7 or MDA-MB-231 cells were washed, polysome lysis buffer, protease inhibitor, and RNase inhibitor were added to the cell pellet. DNA was removed from the mixture, and divided into three groups (IP, IgG, Input). Anti-pan-ago antibody (Millipore, Cat#MABE56) in the Input group, or negative control (NC) IgG antibody in the IgG group were rotated overnight respectively with Protein G magnetic beads at 4°C for 1 hour. After the beads were washed, they were dissolved in TRIzol for the downstream RNA analysis.

2.6 Cell proliferation assay (clone formation, CCK8 and EdU assays), cell apoptosis analysis, and dual-luciference reporter assay

A total of 500 cells were cultured in each well of a six-well plate (Corning, USA). The wells were washed with PBS after two weeks followed by fixation with paraformaldehyde for 15 min. Finally the wells were stained with 0.2% crystal violet for 10 min and washed with running water.

A total of 2000 cells were cultured in each well of ninety-six wells plate. CCK8 was added to the wells at different time points as mentioned. After the samples were incubated at 37°C for 2 hours and the medium was removed, add the color liquid to it and incubate again for 15 min. Read the OD values at 490 nm.

A total of 1×10^5 cells were cultured in each well of ninety-six wells plates. DNA synthesis was evaluated with a Cell-Light EdU In Vitro Kits and DAPI, which were purchased from RiboBio (Guangzhou, China). The experiment was performed according to the protocol.

A total of 5×10^5 cells were concentrated and washed with PBS. After staining with Annexin V-APC and 7-aminoactinomycin D, the apoptotic cell rates were detected by flow cytometry (BD).

A total of 2×10^5 HEK293T cells were cultured in twelve-well plates one day in advance. Two micrograms of the constructed vector with mimics was co-transfected into the cells using Lipo2000. The cells were dissolved in the buffer and assayed for dual-luciferase activity after transfection for 24 h using Dual-Luciferase Assay Kits (Promega, USA).

2.7 Xenograft tumour assay

MCF7 cells (5 × 106) stably overexpressing 5-tRF-His as indicated were injected hypodermically into 8-week-old athymic nude mice (Modong, China). The animal

experiments were performed with the approval of the Ethics Committee of Nanjing Medical University [NO.840 (2019)] and the researchers abided by the laws and policies.

2.8 Statistical analysis

All data are represented as the mean with standard error, and the experiments were carried out in triplicate. SPSS 20.0 and GraphPad Prism 7.0 software were used for analysis. The statistical significance was represented as P<0.05, **P<0.01 or ***P<0.001 was defined as a significant.

3. Results

3.1 Downregulation of 5-tRF-His in BC tissues and cells

We have previously identified a subset of tRFs [9], and therefore, further studies of the published data were performed to describe the characteristic sequence of the tRF-5 type, named 5-tRF-His. Notably, 5-tRF-His has not been shown to be dysregulated in human cancers.

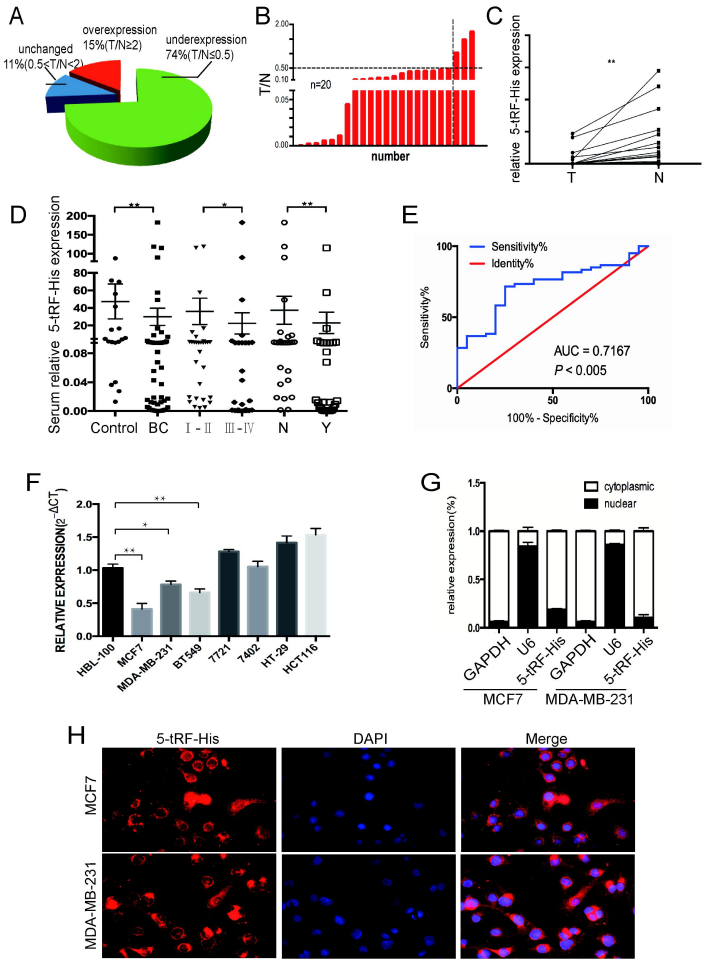

Figure 1. Strong downregulation of 5-tRF-His is observed in BC tissues and cells. (A) The ratio of 5-tRF-His expression in the human BC and corresponding normal tissue pairs (T/N) is grouped into three groups by T/N=2 and 0.5 in the pie graph. (B) Twenty-three pairs are divided into two groups by T/N=0.5 (black dotted line in the X direction). The ratio of twenty pairs was below 0.5 (left of the black dotted in the Y direction) and that of the other three pairs was more than 0.5-fold and less than 2-fold (right of the black dotted in the Y direction). (C) Relative expression of 5-tRF-His from the human BC (T) and corresponding adjacent tissue (N) is accessed by qRT-PCR (n=23). (D) Scatter diagram of serum 5-tRF-His in the normal healthy controls and the BC patients. U6 is used as an internal reference. * $P< 0.05$; ** $P< 0.01$ (E) Receiver operating characteristic(ROC) curves from serum 5-tRF-His in detecting BC.(F) Relative expression of 5-tRF-His in a human normal breast cell line (HBL-100), BC cell lines (MCF7, MDA-MB-231, BT549), liver cancer cells (SMMC-7721, Bel-7402) and colorectal cancer cells (HT-29, HCT116) is measured by qRT-PCR. (G) 5-tRF-His is measured by qRT-PCR in the extracts from the nucleus and cytoplasm of BC cells. (H) Subcellular location of 5-tRF-His in the MCF7 and MDA-MB-231 cells as determined by ISH assays. The nucleus is stained with DAPI. 5-tRF-His was detected by a cy3-lablled probe.

The expression of 5-tRF-His was detected in twenty-seven paired BC tissues and adjacent tissues by qRT-PCR. Consistent with the sequencing data, the results from the whole paired tissues, which were standardized with U6, revealed that 5-tRF-His was decreased in 74%(20/27) of the cancer specimens compared with the adjacent samples (Fig.1A-C). Additionally, we measured the 5-tRF-His level in the serum samples from sixty BC patients and twenty healthy controls. As shown in Fig. 1D, 5-tRF-His was decreased in the patients related to the controls, and low expression of serum 5-tRF-His was significantly related to TNM stage III-IV and lymph node metastasis. These findings indicated that the downregulation of 5-tRF-His was related to BC development. To detect the diagnostic value of 5-tRF-His, we analyzed the area under the ROC curve. Then 5-tRF-His was proved to be a diagnostic molecule (AUC=0.7167, $P<0.005$) (Fig. 1E). Therefore, we highlight the availability of our sequencing method.

Next we performed qRT-PCR to explore 5-tRF-His expression in a human normal breast cell line (HBL-100), BC cell lines (MCF7, MDA-MB-231, BT549), liver cancer cells (SMMC-7721, Bel-7402) and colorectal cancer cells (HT-29, HCT116). The data demonstrated that 5-tRF-His was substantially lower in the BC cell lines than that in the other cell lines (Fig. 1F), and among the BC cells, the high-expression MDA-MB-231 and the low-expression MCF7 was selected as basic tools to study for the next experiments. qRT-PCR of fractions from the nucleus and cytoplasm showed that 5-tRF-His was expressed at higher level in the cytoplasm than in the nucleus. Fluorescence ISH assays were also used to explore the subcellular distribution of 5-tRF-His, and the results was corresponded with the qRT-PCR assay (Fig. 1G and H), indicating that 5-tRF-His could have an active impact at the post-transcriptional level.

3.2 The correlation between 5-tRF-His and clinicopathological characteristics

Next, we explored the correlation between 5-tRF-His and the clinicopathological characteristics of the twenty-seven paired tissues. The qRT-PCR results showed that the low expression of 5-tRF-His was related to lymph node metastasis (p=0.0284) but not age, tumor size, TNM stage, or differentiation (Tab. 1).

Table1. The correlation between 5-tRF-His and the clinicopathological characteristics

		5-tRF-His		*P* value
characteristics	**n**	**Low**	**High**	
Number				
Age				
<50	12	4	8	0.6960
≥50	15	7	8	
Tumor size(cm)				
<4	17	6	11	0.6868
≥4	10	5	5	
Lymphnode metastasis				
yes	16	5	11	0.0284
no	11	9	2	
TNM stage				
Ⅰ-Ⅱ	13	3	10	0.0542
Ⅲ-Ⅳ	14	9	5	
differentiation				
well	9	3	6	
moderate	8	5	3	
poor	10	5	5	0.4807

3.3 The 5-tRF-His molecule linked to pan-ago, as a tRNA-derived fragment

The molecule 5-tRF-His belongs to a class of 23-nt small RNAs and the sequences is 5'-TGCCGTGATCGTATAGTGGTTAG-3'. The unique ID in MINTBase is tRF-23-XSXMSL730H. After searching the website (https://cm.jefferson.edu/MINTbase/) [17], we found that the fragments matched perfectly to the 5' end of at least nine annotated tRNAs and the cleavage site of the D loop was detected in these sequences. The precursor RNA carried the amino acid histidine by the anticodon GTG, and thus the cleaved fragment was named 5-tRF-His according to previous studies (Fig. 2A and B).

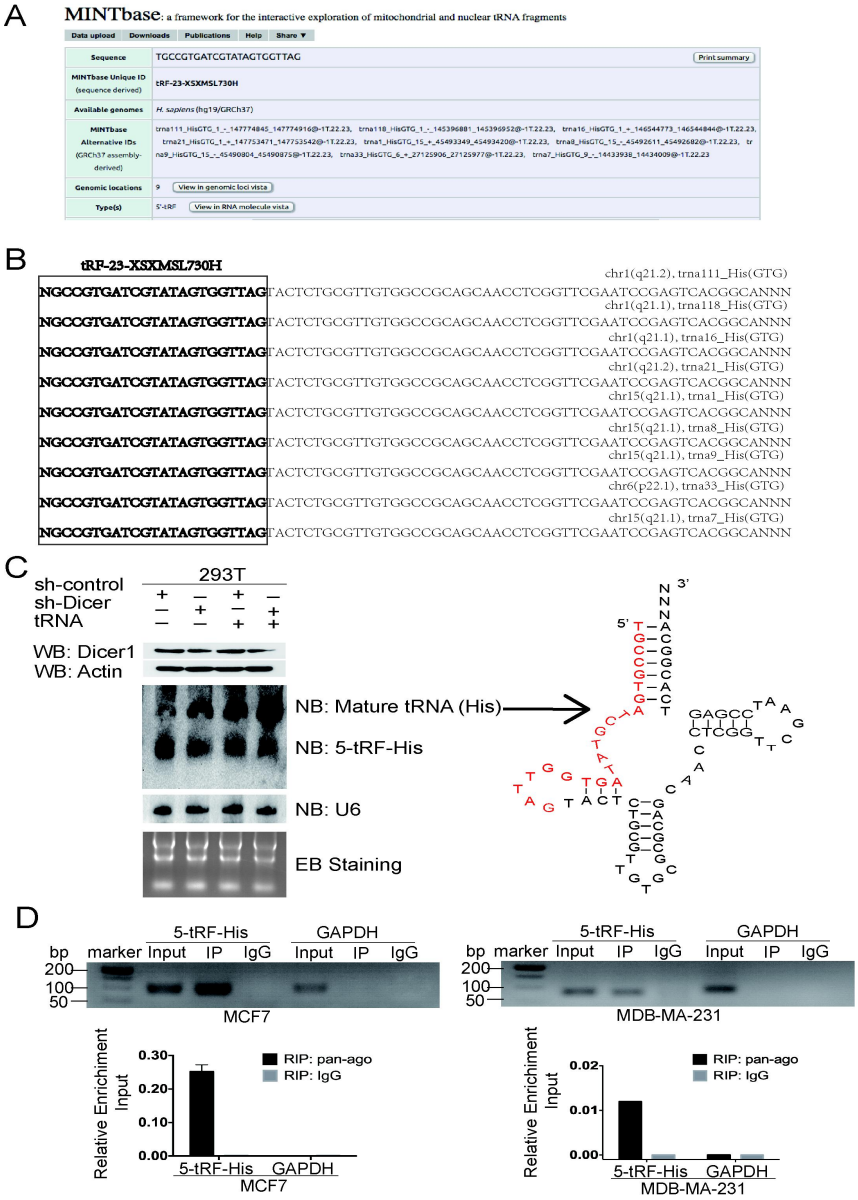

Figure 2. The 5-tRF-His molecule linked to pan-ago is a tRNA-derived fragment. (A) The MINTBase Unique ID of 5-tRF-His is tRF-23-XSXMSL730H, with nine genomic locations as a type of 5'-tRF. Detailed items are searched in MINTBase, https://cm.jefferson.edu/MINTbase/. (B) Sequences of the 5-tRF-His small RNA and the nine chromosomal locations separately. The 5-tRF-His sequences are in bold in the textbox. (C) Levels of Dicer protein and total RNA are detected by western blot (WB) and northern blot (NB) in the 293T cells stably transfected with control shRNA or Dicer1-targeting shRNA (shDicer1) and transiently transfected with empty or His (GTG) mature tRNA. The 5-tRF-His molecule, with a length of 23 nt, is derived from the 5' end of the mature tRNA-His-GTG with 76 nucleotides. Actin was used as a control in WB, with U6 and ethindium bromide (EB) staining in NB. (D) The 5-tRF-His bound to the pan-ago protein plays an important role as a miRNA. The IP of 5-tRF-His and pan-ago protein and qRT-PCR of 5-tRF-His in the IP fractions of in MCF7 and MDA-MB-231 cells are shown. Nonspecific IgG was used as the isotype control antibody. Error bars represent the SD of three independent experiments.

Here we hypothesized that 5-tRF-His was synthesized in a classical Dicer1-dependent manner owing to its similar to the size of miRNA [18]. To verify the relationship among 5-tRF-His, tRNAs and Dicer1, we cloned 5-tRF-His-matching tRNA sequences in a plasmid and transferred the cloned plasmid into 293T cells with stable knockdown of Dicer1. Northern blot analysis showed that the knockdown of Dicer1 was essential for the reduced biogenesis of 5-tRF-His and the accumulation of mature tRNA (Fig. 2C). The results indicated that Dicer1 was involved in the cleavage of mature tRNA, resulting in the production of 5-tRF-His.

Many researchers now have focused on the underlying function of tRFs, which are members of Argonaute complexes, indicating their miRNA-like activities [19-20]. We wondered if 5-tRF-His was related to the enzyme Argonaute. Through affinity to a pan-ago antibody against four human proteins of Argonaute, we purified the antibody-bound RNA from MCF7 and MDA-MB-231 cells. The qRT-PCR data shown that 5-tRF-His was physically enriched in the IP extraction compared with that of the control IP (Fig. 2D), suggesting that 5-tRF-His combined with Argonaute proteins as a prerequisite condition and may impact effectors in a manner similar to that of miRNA.

3.4 Effects of 5-tRF-His on proliferation and apoptosis in BC cells

To confirm whether the expression of 5-tRF-His can inhibit the proliferation of BC cell lines, we designed mimics to perform cell proliferation assays. After transiently transfecting MCF7 and MDA-MB-231 cells with mimics or NC, we detected a more than 20-fold increase in 5-tRF-His relative to that of the NC group (Fig. 3A). CCK8 assays showed that the overexpression of 5-tRF-His substantially reduced the cell proliferation (Fig. 3B). Colony formation and EdU assays also showed that the 5-tRF-His subclone formed few colonies and contained less EdU than the NC subclone (Fig.3C and D). The flow cytometry results demonstrated that 5-tRF-His overexpression promoted apoptosis in the MCF7 and MDA-MB-231 cells (Fig. 3E), indicating that 5-tRF-His functioned as a tumor suppressor in vitro.

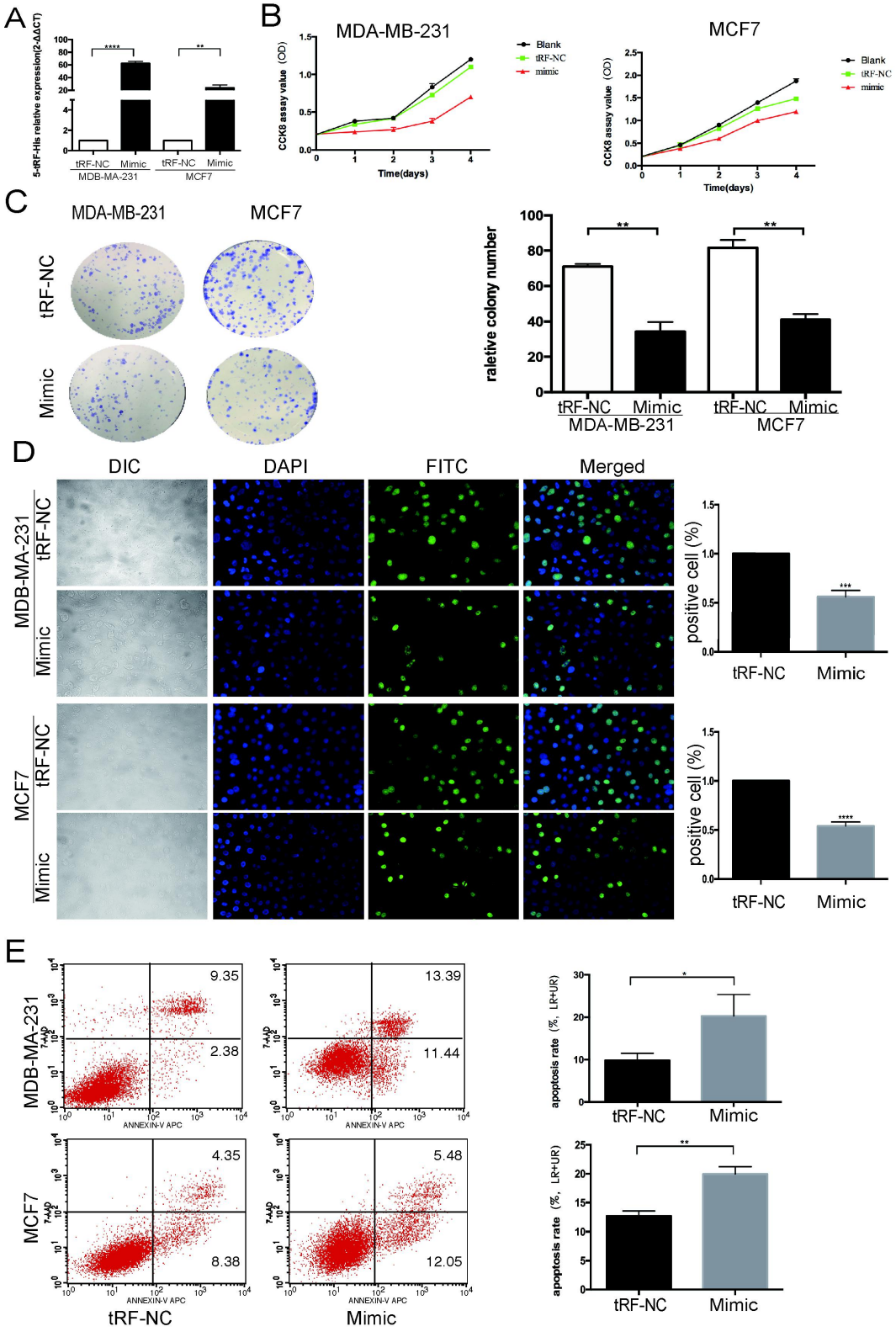

Figure 3. The 5-tRF-His molecule regulates the proliferation and apoptosis of BC cells. (A) The transient expression of 5-tRF-His in the MDB-MA-231 and MCF7 cells transfected with NC or 5-tRF-His mimic was measured by qRT-PCR. (B) CCK8 assays are carried out to measure the proliferation of the MDB-MA-231 and MCF7 cells. (C and D) 5-tRF-His reduces the proliferation in the colony formation and EdU assays. (E) Cell apoptosis in the treated MDB-MA-231 and MCF7 cells is detected by flow cytometry.

3.5 Effect of 5-tRF-His on tumor growth in the explant tumor of mice

To further explore the function of 5-tRF-His in BC tumorigenesis, we subcutaneously injected the MCF7 cells stably transfected with lentivirus overexpressing 5-tRF-His (LV-tRF) or control (LV-control) into nude mice. As shown in Fig. 4A, xenograft mouse models were generated. The weights of the nude mice and the explant tumors in the LV-tRF group were both significantly lower than those in the LV-control group (Fig. 4B and C). Moreover, staining of Ki67, which is a proliferative marker, was decreased, as shown by fluorescence ISH, while 5-tRF-His was overexpressed relative to that in the control (Fig. 4D and E).

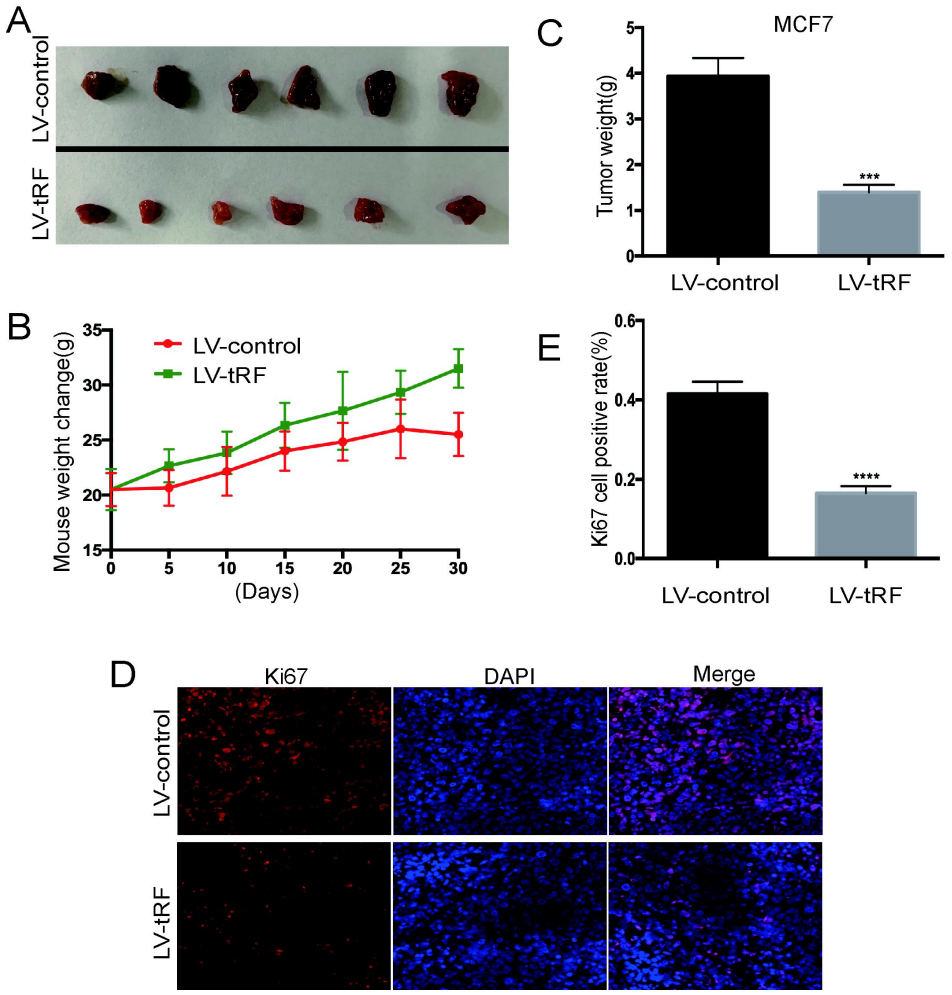

Figure 4. The 5-tRF-His mediates inhibition of BC tumor growth in the explant tumor of mice (n=5 per group). (A) Images of the nude mice injected with MCF7 cells stably expressing 5-tRF-His/LV-tRF or NC/LV-control (n=6) Explant tumors separated from the mice in the two groups. (B) The weights of the nude mice injected with MCF7/LV-control and MCF7/LV-tRF are assessed for 30 days and graphed to generate the tumor growth curves every five days (two-way ANOVA test). (C) Explant tumor weight of the nude mice injected with MCF7/LV-control and MCF7/LV-tRF (Student's t-test). ***P<0.001. (D) Representative fluorescence ISH images showing Ki67 (red) and DAPI (blue) in the tumor tissues of the two groups. (E) Quantitative analysis of the Ki67-positive cells show a substantially lower in the nude mice injected with MCF7 cells stably expressing 5-tRF-His than the mice inoculated with control. ****P < 0.0001.

3.6 5-tRF-His acts as a miRNA and is directly negatively related to CKAP2

Considering that tRFs were previously shown to be similar to sponge-like miRNAs in some studies and that 5-tRF-His was primarily located in the cytoplasm, we searched TargetScan and miRBase to predict potential target genes and found that CKAP2 may directly bind to 5-tRF-His. We further analyzed TCGA data and demonstrated that CKAP2 was significantly overexpressed in BC and that patients with low CKAP2 expression did not have an improved prognosis (p=0. 321, Fig. 5A and B). Then, dual-luciferase reporter assays were carried out, and the results showed that 5-tRF-His strongly inhibited the luciferase activity of the wild-type sequence in 293T cells (Fig. 5C). The mRNA and protein expression of CKAP2 in MCF7 and MDA-MB-231 cells was abundantly decreased after transfection with 5-tRF-His mimics compared with the NC. In western blot analysis, we also found that overexpression of 5-tRF-His reduced the protein levels of PCNA and p-ERK2, regardless of the expression of ERK2 (Fig. 5D and E). To further explore the relationship between 5-tRF-His and CKAP2, we performed TMA analysis, which showed a significantly negative association between the two molecules in BC (n=132)(Fig. 5F and G). In the postoperative follow-up survey, we merged two groups of BC patients whose tumoral 5-tRF-His expressions were categorized as '++' (n=18) and '+++' (n=37) and analyzed data from the groups categorized as '+' (n=77) and '++~+++' (n=55). Fig. 5H showed that those with low 5-tRF-His expressions (+) had shorter survival days than those with high 5-tRF-His expressions (++~+++) (P=0.0084).

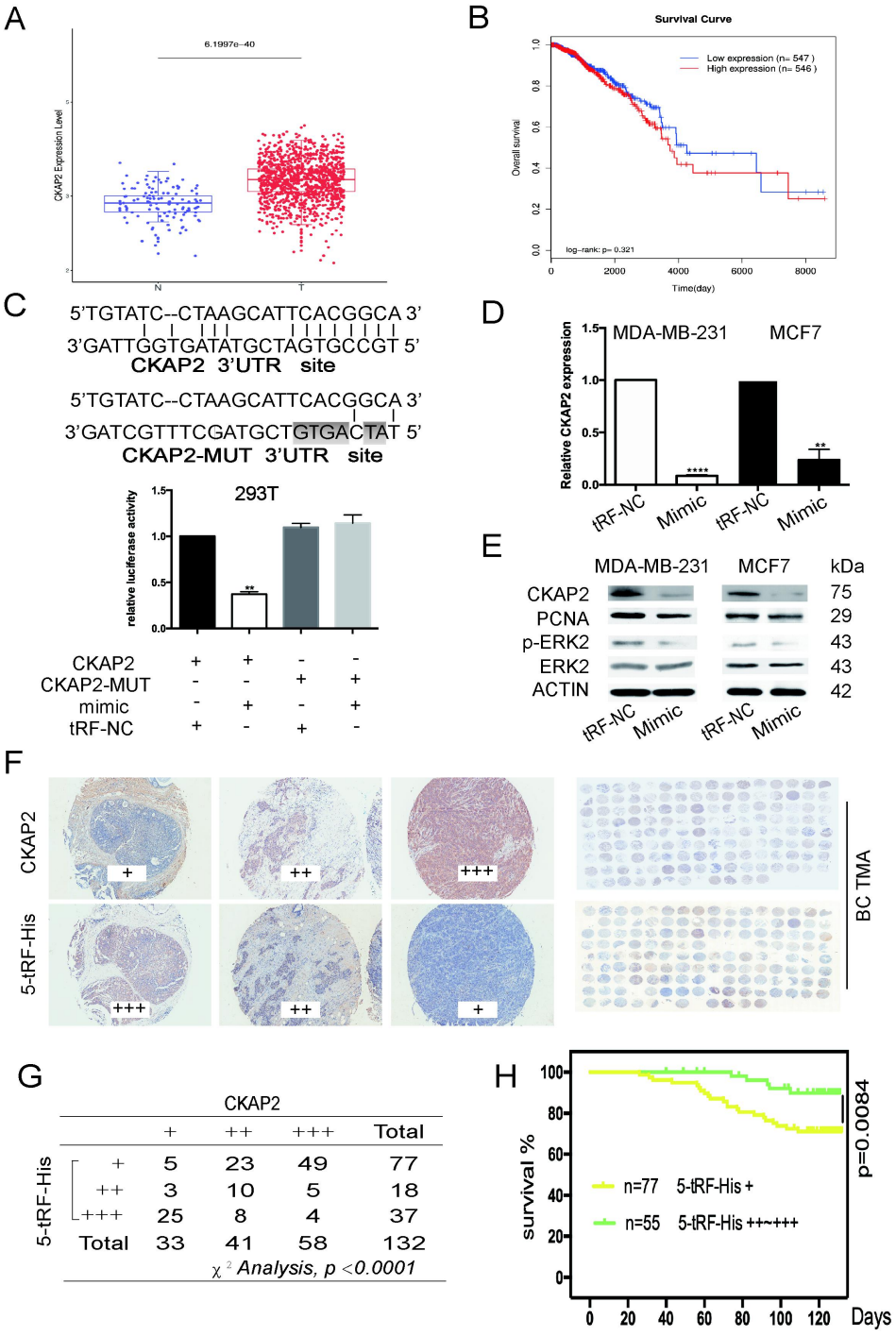

Figure 5. The 5-tRF-His molecule acts as a miRNA and is directly negatively related to CKAP2, which is overexpressed in BC tissues. (A) The expression level of CKAP2 in BC is analyzed by TCGA data, P<0.0001. (B) The prognosis of CKAP2 in BC patients is shown in TCGA data. P =0.321. (C) A schematic diagram of the 3'UTR of the CKAP2 mRNA targeted by 5-tRF-His is shown, as well as the mutant sequences of the 3'UTR. Dual-luciferase reporter assays validate the predicted binding site. (D) qRT-PCR is performed to transiently measure the relative mRNA level of CKAP2 in the MDB-MA-231 and MCF7 cells treated with tRF-NC or 5-tRF-His mimic. (E) WB analysis reveals decreased expression of CKAP2, PCNA and p-ERK2 in the 5-tRF-His mimic-treated cells compared with the tRF-NC-treated cells. (F) Representative IHC images of CKAP2 and 5-tRF-His staining from the TMA. (G) And a chi-square test is conducted to analyze the data. (H) Survival analyze of BC patients with different expressions of 5-tRF-His in a 140-day postoperative follow-up survey.

3.7 5-tRF-His regulates proliferation and apoptosis in an erk2-dependent manner

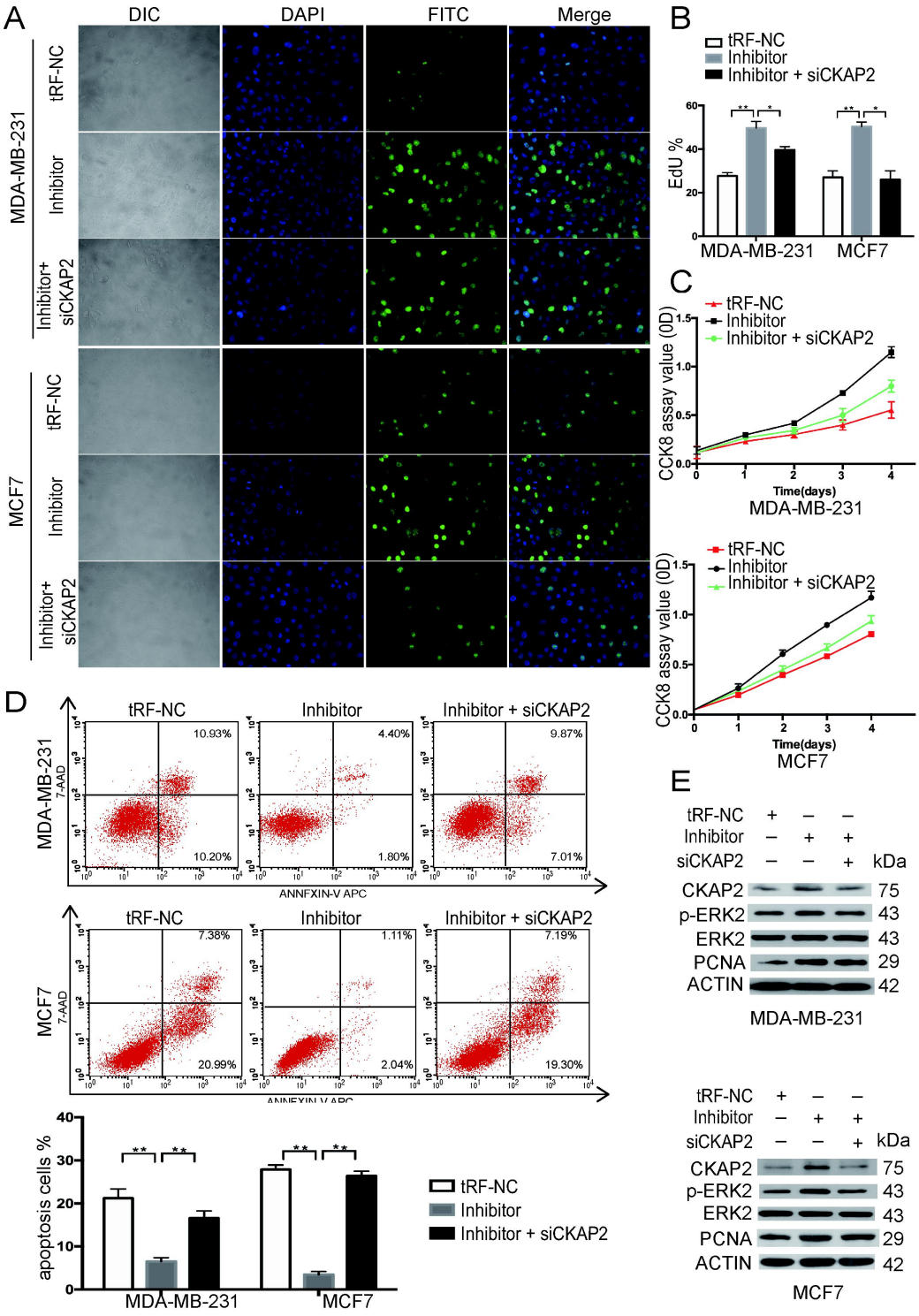

Figure 6. The 5-tRF-His molecule regulates proliferation and apoptosis in an erk2-dependent manner. (A-C) The proliferation of the transfected MDB-MA-231 and MCF7 cells is detected by EdU and CCK8 assays. (D) Flow cytometry is performed to measure the cell apoptosis rates of the rescued MDB-MA-231 and MCF7 cells. (E) Western blot assays are used to measure the associated protein levels in the treated MDB-MA-231 and MCF7 cells.

The results above demonstrated that the 3'UTR of CKAP2 matched the binging site of 5-tRF-His directly, suggesting that 5-tRF-His might competitively regulate CKAP2 expression. Previous reports showed that CKAP2 induced the proliferation of BC cells in an ERK2-dependent manner [12]. We hypothesized that 5-tRF-His regulated cell proliferation and apoptosis through the CKAP2 signal pathway. The expression of CKAP2 was downregulated via siRNAs specially targeting CKAP2, and then, rescued experiments were performed. We simultaneously transfected the 5-tRF-His inhibitor into the MDB-MA-231 and MCF7 cells with si-CKAP2. The increase in the number of EdU-stained cells induced by the inhibitor was reversed by si-CKAP2, as shown in EdU assays (Fig. 6A and B). CCK8 assays revealed that inhibition of 5-tRF-His increased cell proliferation. Nevertheless, the promotion was locally rescued by the low coexpression of CKAP2 (Fig. 6C). Moreover, the decreasing number of apoptotic cells produced by 5-tRF-His inhibitor was also confirmed reversed by si-CKAP2. Western blot showed that downexpression of CKAP2 could rescue the protein levels of downstream target genes, such as p-ERK2 and PCNA, regardless of the expression of ERK2, suggesting that the effect of 5-tRF-His on cell proliferation and apoptosis was mediated by CKAP2 in the ERK2 signaling pathway (Fig. 7).

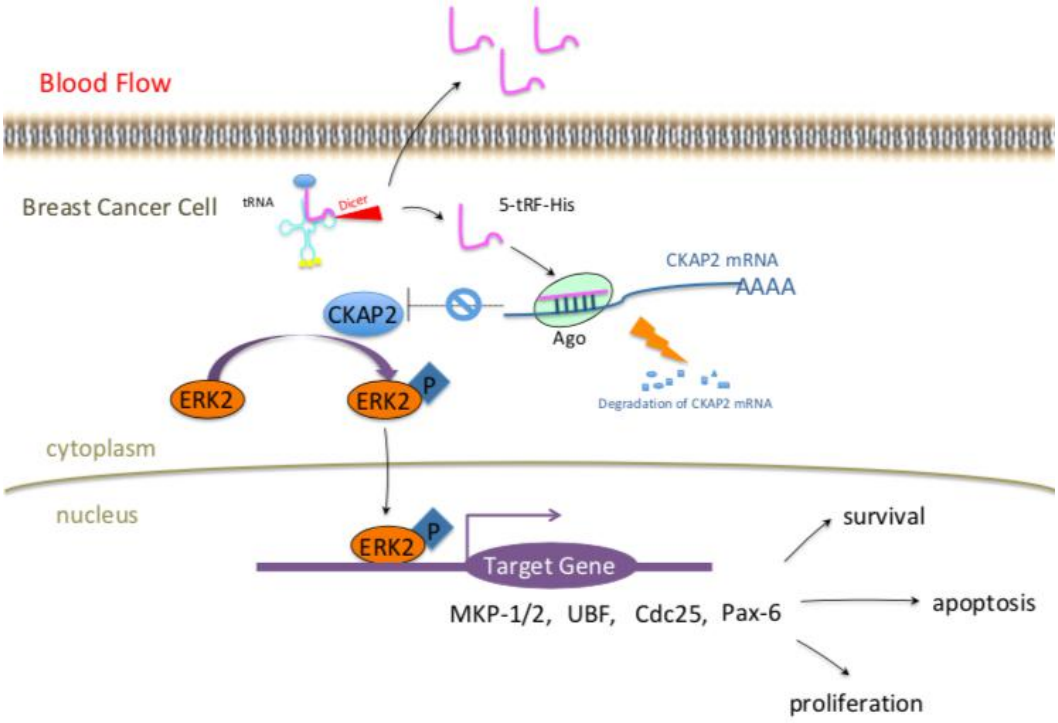

Figure 7. Possible mechanism of 5-tRF-His molecule: regulating CKAP2 directly to control erk2 signalling pathway by function like a miRNA in BC cells.

4. Discussion

Improvements in next-generation sequencing technology have allowed researchers to identify the altered profile of noncoding RNAs in human cancers. Many studies have uncovered that miRNAs, lncRNAs and circRNAs frequently function in tumor heterogeneity [21-23]. Nevertheless, the expression and effect of tRFs in tumors were still known little during the last decade [24, 25]. As our group has previously reported tRFs in BC [9], we speculated that one of these tRFs, 5-tRF-His might influence on BC as well. Here we studied that the expression of 5-tRF-His was remarkably decreased comparing BC tissues with adjacent breast tissues (Fig.1A-C), which implied a functional role in the biological progress of tumorigenesis of BC. Also, we concentrated on 5-tRF-His in the blood, which was extremely down regulated in the serum of BC patients compared to healthy controls (Fig.1D-E).

Given the traditional role of these molecules in carrying amino acids into ribosomes and elongating peptide chains guided by mRNAs, we observed that tRFs can participate in the progression of cell growth through various mechanisms, such as involving inhibiting the stable transcripts via YBX1 displacement of 3'UTRs [26], mediating transposon reactivation by suppressing endogenous retrovirus families [27], and repressing immune activation partially released by multivesicular bodies in T cells [28]. The published studies described here have further demonstrated the regulatory capability of the fragments and enriched the expression profile of miRNA-like small RNAs, implying that tRFs could target downstream genes post-transcriptionally in a site-specific fashion.

Researchers have shown that tRFs are actively derived from precursor RNAs and that the 3' or 5' end-matching tRFs are largely cleaved by Dicer1 owing to their structural features, which are similar to those of miRNA [29]. Dicer1 is a widely known RNase involved in miRNA activities [30]. Here we used similar approaches to verify that Dicer1 is essential for the production of 5-tRF-His. ShRNA inhibition of Dicer1 was confirmed by western blots and the results demonstrated that following knockdown of Dicer1, accumulation of mature RNAs and exhaustion of 5-tRF-His were detected in northern blot (Fig. 2C). Interestingly, a functional resemblance was also found in the binding to pan-ago proteins in BC cell inclusions (Fig. 2D). Then we verified that 5-tRF-His could inhibit BC cell proliferation in vivo and in vitro (Fig. 3 and 4). The subcellular location of 5-tRF-His was in the breast cell cytoplasm, implying that it was regulated at the post-transcriptional level (Fig. 1F and G). The expression of CKAP2 in BC cells has already been reported to play its critical role in inducing

proliferation [14]. Thus, 5-tRF-His could directly target mRNA in an ago-dependent manner, and the targeted site was identified in the 3'UTR of CKAP2 mRNA (Fig.5).

CKAP2 is a required molecule of stabilizing microtubules for the regulation of cell growth, and it has already been studied in many cancer cells. As an effective oncogene in human cancers, CKAP2 has also been studied in BC and little is known concerning its regulation at post-transcriptional level regulated by 5-tRF-His. Therefore, we detected the protein level of CKAP2 using an inhibitor of 5-tRF-His to help elucidate the carcinogenic mechanism in BC. The FAK-ERK2 signalling pathway is the leading downstream pathway of CKAP2 [12, 31]. Coincidentally, our data proved that increasing 5-tRF-His strongly downregulated the protein expression of p-ERK2 and PCNA. Furthermore, the interaction with 5-tRF-His CKAP2 mRNA reduced the proliferation of BC cells, inhibiting the downstream expression of p-ERK2 and PCNA (Fig. 6).

The findings in this study have not fully elucidated the effects of 5-tRF-His expression and the mechanisms of its functional targets. Future studies about this class of fragments will be performed and the development of therapeutic methods related to 5-tRF-His should be undertaken.

5. Conclusions

In summary, we represent that 5-tRF-His plays an important role in BC development. Mechanically, the 5-tRF-His molecule regulates BC cells through CKAP2 in an ERK2-dependent manner. Also, the binding to pan-ago proteins of 5-tRF-His might be a tumor growth mechanism, influencing many biological processes that worth exploring further.

Author Contributions: YF: design and guide the study; TX: conduct most of the experiments and complete the manuscript; JP, CHH, WJ and MDP: do animal researches; XXD, TL and MXL: take charge of the clinical specimen collection and statistics.

Funding: This research was funded by the National Natural Science Foundation of China (81871718), Innovative Team of Jiangsu Province (CXTDA2017017) and the Medical Research Project of Jiangsu Commission of Health (H2019070).

References

[1] Bray F; Ferlay J; Soerjomataram I; Siegel RL; Torre LA; Jemal A. Global cancer statistics 2018: GLOBOCAN estimates of incidence and mortality worldwide for 36 cancers in 185 countries. *CA Cancer J Clin*. 2018, 68, 394-424. DOI: 10.3322/caac.21492

[2] DeSantis CE; Ma J; Goding Sauer A; Newman LA; Jemal A. Breast cancer statistics, 2017, racial disparity in mortality by state. *CA Cancer J Clin.* 2017, 67, 439-48. DOI: 10.3322/caac.21412

[3] Benoit Bouvrette LP; Cody NAL; Bergalet J; Lefebvre; FA; Diot C; Wang X et al. CeFra-seq reveals broad asymmetric mRNA and noncoding RNA distribution profiles in Drosophila and human cells. *RNA* 2018, 24, 98-113. DOI: 10.1261/rna.063172.117

[4] Ta HQ; Whitworth H; Yin Y; Conaway M; Frierson HFJ; Campbell MJ et al. Discovery of a novel long noncoding RNA overlapping the LCK gene that regulates prostate cancer cell growth. *Mol Cancer.* 2019, 18, 113. DOI: 10.1186/s12943-019-1039-6

[5] Martinez G; Choudury SG; Slotkin RK. tRNA-derived small RNAs target transposable element transcripts. *Nucleic Acids Res.* 2017, 45, 5142-52. DOI: 10.1093/nar/gkx103

[6] Lyons SM; Fay MM; Akiyama Y; Anderson PJ; Ivanov P. RNA biology of angiogenin: Current state and perspectives. *RNA Biol.* 2017, 14, 171-8. DOI: 10.1080/15476286.2016.1272746

[7] Kumar P; Kuscu C; Dutta A. Biogenesis and Function of Transfer RNA-Related Fragments (tRFs). *Trends Biochem Sci.* 2016, 41, 679-89. DOI: 10.1016/j.tibs.2016.05.004

[8] Chen Z; Qi M; Shen B; Luo G; Wu Y; Li J et al. Transfer RNA demethylase ALKBH3 promotes cancer progression via induction of tRNA-derived small RNAs. *Nucleic Acids Res.* 2019, 47, 2533-45. DOI: 10.1093/nar/gky1250

[9] Wang X; Yang Y; Tan X; Mao X; Wei D; Yao Y et al. Identification of tRNA-Derived Fragments Expression Profile in Breast Cancer Tissues. *Curr Genomics.* 2019, 20, 199-213. DOI: 10.2174/1389202920666190326145459

[10] Case CM; Sackett DL; Wangsa D; Karpova T; McNally JG; Ried T et al. CKAP2 ensures chromosomal stability by maintaining the integrity of microtubule nucleation sites. *PLoS One.* 2013, 8, e64575. DOI: 10.1371/journal.pone.0064575

[11] Yoo BH; Kang DS; Park CH; Kang K; Bae CD. CKAP2 phosphorylation by CDK1/cyclinB1 is crucial for maintaining centrosome integrity. *Exp Mol Med.* 2017, 49, e354. DOI: 10.1038/emm.2017.92

[12] Guo QS; Song Y; Hua KQ; Gao SJ. Involvement of FAK-ERK2 signaling pathway in CKAP2-induced proliferation and motility in cervical carcinoma cell lines. *Sci Rep.* 2017, 7, 2117. DOI: 10.1038/s41598-017-01832-y

[13] Wang K; Huang R; Li G; Zeng F; Zhao Z; Liu Y et al. CKAP2 expression is associated with glioma tumor growth and acts as a prognostic factor in highgrade glioma. *Oncol Rep.* 2018, 40, 2036-46. DOI: 10.3892/or.2018.6611

[14] Sim SH; Bae CD; Kwon Y; Hwang HL; Poojan S; Hong HI et al. CKAP2 (cytoskeleton-associated protein2) is a new prognostic marker in HER2-negative luminal type breast cancer. *PLoS One.* 2017, 12, e0182107. DOI: 10.1371/journal.pone.0182107

[15] Tang X; Chen X; Xu Y; Qiao Y; Zhang X; Wang Y et al. CD166 positively regulates MCAM via inhibition to ubiquitin E3 ligases Smurf1 and betaTrCP through PI3K/AKT and c-Raf/MEK/ERK signaling in Bel-7402 hepatocellular carcinoma cells. *Cell Signal.* 2015, 27, 1694-702. DOI: 10.1016/j.cellsig.2015.05.006

[16] Wang J; Tang X; Weng W; Qiao Y; Lin J; Liu W et al. The membrane protein melanoma cell adhesion molecule (MCAM) is a novel tumor marker that stimulates tumorigenesis in hepatocellular carcinoma. *Oncogene* 2015, 34, 5781-95. DOI: 10.1038/onc.2015.36

[17] Loher P; Telonis AG; Rigoutsos I. MINTmap: fast and exhaustive profiling of nuclear and mitochondrial tRNA fragments from short RNA-seq data. *Sci Rep.* 2017, 7, 41184. DOI: 10.1038/srep41184

[18] Maute RL; Schneider C; Sumazin P; Holmes A; Califano A; Basso K et al. tRNA-derived microRNA modulates proliferation and the DNA damage response and is down-regulated in B cell lymphoma. *Proc Natl Acad Sci U S A.* 2013,110, 1404-9. DOI: 10.1073/pnas.1206761110

[19] Huang B; Yang H; Cheng X; Wang D; Fu S; Shen W et al. tRF/miR-1280 Suppresses Stem Cell-like Cells and Metastasis in Colorectal Cancer. *Cancer Res.* 2017, 77, 3194-206. DOI: 10.1158/0008-5472.CAN-16-3146

[20] Mo D; Jiang P; Yang Y; Mao X; Tan X; Tang X et al. A tRNA fragment, 5'-tiRNA(Val), suppresses the Wnt/beta-catenin signaling pathway by targeting FZD3 in breast cancer. *Cancer Lett.* 2019, 457,60-73. DOI: 10.1016/j.canlet.2019.05.007

[21] Hydbring P; Wang Y; Fassl A; Li X; Matia V; Otto T et al. Cell-Cycle-Targeting MicroRNAs as Therapeutic Tools against Refractory Cancers. *Cancer Cell.* 2017, 31, 576-90 e8. 10.1016/j.ccell.2017.03.004

[22] Yang Y; Chen L; Gu J; Zhang H; Yuan J; Lian Q et al. Recurrently deregulated lncRNAs in hepatocellular carcinoma. *Nat Commun.* 2017, 8, 14421. DOI: 10.1038/ncomms14421

[23] Vo JN; Cieslik M; Zhang Y; Shukla S; Xiao L; Zhang Y et al. The Landscape of Circular RNA in Cancer. *Cell* 2019, 176, 869-81 e13. DOI: 10.1016/j.cell.2018.12.021

[24] Telonis AG; Loher P; Magee R; Pliatsika V; Londin E; Kirino Y et al. tRNA Fragments Show Intertwining with mRNAs of Specific Repeat Content and Have Links to Disparities. *Cancer Res.* 2019, 79, 034-49. DOI: 10.1158/0008-5472.CAN-19-0789

[25] Roura Frigole H; Camacho N; Castellvi Coma M; Fernandez-Lozano C; Garcia-Lema J; Rafels-Ybern A et al. tRNA deamination by ADAT requires substrate-specific recognition mechanisms and can be inhibited by tRFs. *RNA* 2019, 25, 607-19. DOI: 10.1261/rna.068189.118

[26] Goodarzi H; Liu X; Nguyen HC; Zhang S; Fish L; Tavazoie SF. Endogenous tRNA-Derived Fragments Suppress Breast Cancer Progression via YBX1 Displacement. *Cell* 2015, 161, 790-802. DOI: 10.1016/j.cell.2015.02.053

[27] Schorn AJ; Gutbrod MJ; LeBlanc C; Martienssen R. LTR-Retrotransposon Control by tRNA-Derived Small RNAs. *Cell* 2017, 170, 61-71. DOI: 10.1016/j.cell.2017.06.013

[28] Chiou NT; Kageyama R; Ansel KM. Selective Export into Extracellular Vesicles and Function of tRNA Fragments during T Cell Activation. *Cell Rep.* 2018,25,3356-70 e4. DOI: 10.1016/j.celrep.2018.11.073

[29] Kuscu C; Kumar P; Kiran M; Su Z; Malik A; Dutta A. tRNA fragments (tRFs) guide Ago to regulate gene expression post-transcriptionally in a Dicer-independent manner. *RNA* 2018, 24, 1093-105. DOI: 10.1261/rna.066126.118

[30] Vedanayagam J; Chatila WK; Aksoy BA; Majumdar S; Skanderup AJ; Demir E et al. Cancer-associated mutations in DICER1 RNase IIIa and IIIb domains exert similar

effects on miRNA biogenesis. *Nat Commun*. 2019, 10, 3682. DOI: 10.1038/s41467-019-11610-1

[31] Zhang M; Zhao L. CKAP2 Promotes Ovarian Cancer Proliferation and Tumorigenesis Through the FAK-ERK Pathway. *DNA Cell Biol*. 2017, 36, 983-90. DOI: 10.1089/dna.2017.3876